Arabian Journal of Chemistry (2015) **8**, 168–173

King Saud University

Arabian Journal of Chemistry

www.ksu.edu.sa
www.sciencedirect.com

ORIGINAL ARTICLE

Effects of influence of carbon ring-doping on NMR parameters of boron phosphide nanotubes: A DFT study

M. Rezaei-Sameti *

Department of Applied Chemistry, Faculty of Science, Malayer University, Malayer 65174, Iran

Received 22 September 2010; accepted 6 October 2010
Available online 15 February 2011

KEYWORDS

BPNTs;
Chemical shielding;
DFT;
Carbon ring doping

Abstract The electronic structure of boron phosphide nanotubes (BPNTs) and influence of carbon ring doping (C-doping) in the horizontal region (model A) and vertical region (model B) of BPNTs is studied by density functional theory (DFT). At first, each form was optimized at B3LYP level of theory using 6-31G* bases set. After, the computed chemical shielding (CS) tensors at the sites of ^{11}B and ^{31}P nuclei were converted to isotropic chemical shielding (CSI) and anisotropic chemical shielding (CSA). The calculated results reveal that the CS parameters of B and P nuclei in C-ring doped on vertical region (model B) undergo more significant changes than horizontal region (model A).

1. Introduction

In recent years carbon nanotubes (CNTs) have became one of significant topics in the research of nanomaterial science for their unique geometry, band structures, as well as the outstanding mechanical, electrical, thermal, optical properties, molecular device and biosensor (Shen, 2009; Mirzaei and Giahi, 2010; Li et al., 2006; Mirzaei, 2009a,b). Nanotubes consisting of combinations of atoms of groups three and five of the periodic table of elements have been viewed as proper candidates instead of the CNTs (Seif et al., 2007; Mirzaei et al., 2008a,b; Zhang and Zhang, 2003). The properties of group three nitrides have been studied more than those of group III phosphide. Whereas BNNTs, which have much wider energy, band gaps weakly depending on the diameter, chirality, and the number of the walls of the tube, are semiconductors, BNNTs are very attractive materials for application in nanoscale devices (Mpourmakis and Froudakis, 2007; Zhang et al., 2006; Zhou et al., 2002; Baughman et al., 1999; Harris, 1999). The considerable efforts dedicated to the synthesis of non-carbon nanotubes with properties independent of tubular diameter and chirality led to the conclusion that the group III nitrides, especially boron and aluminum nitrides (BN and AlN), are proper materials (Loiseau et al., 1996; Chen et al., 2005; Blase et al., 1994). The stable tubular structures of the nanotubes of BN (Guo et al., 2006; Chopra et al., 1995), were initially characterized by the calculations and then were successfully synthesized by the experiments (Loiseau

---

* Tel./fax: +98 851 3339843.
E-mail address: mrsameti@gmail.com.

Peer review under responsibility of King Saud University.

Production and hosting by Elsevier

http://dx.doi.org/10.1016/j.arabjc.2010.10.035

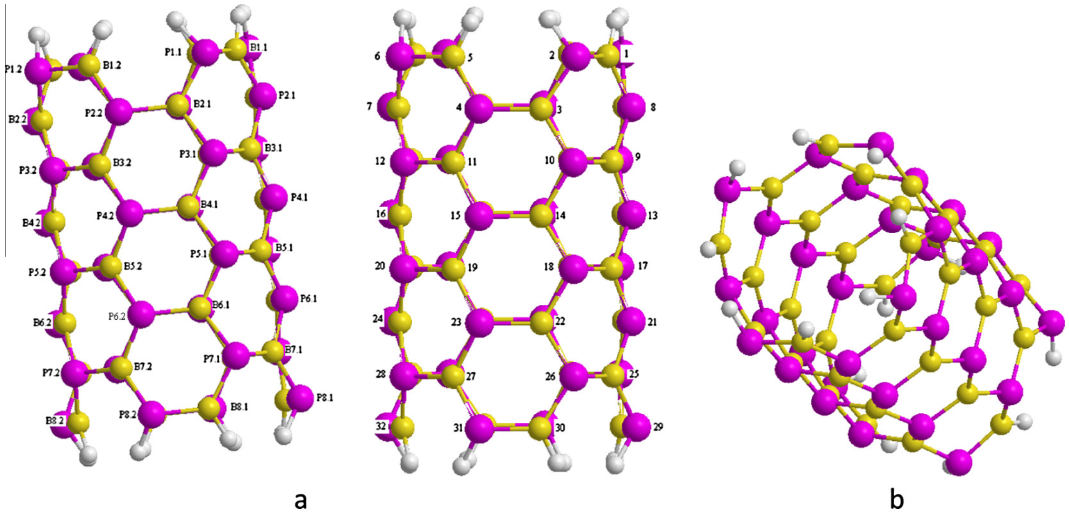

Figure 1 (a) 2D and (b) 3D views of the pristine model of BPNTs.

et al., 1996; Sieh et al., 1995; Oku, 2002; Arenal et al., 2006; Nirmala and Kolandaivel, 2007; Mirzaei, 2009a,b). The similarity between electronic properties of boron phosphide (BP) and silicon carbide (SiC) has made BP nanotube (BPNT) as an important subject of numerous studies (Mirzaei, 2010; Schroten et al., 1998; Ferreira and Leite Alves, 2008). In this computational research, at first time, the properties of the electronic structure and chemical shielding parameters of the armchair (4,4) BPNTs and influence of carbon ring doping (C-doping) on the vertical and horizontal region of this nanotubes (Figs. 1 and 2) have been investigated by performing density functional theory (DFT) calculations of the NMR parameters. At first, the pristine and the C-doped ring structures have been allowed to relax by all atomic geometrical optimization. Subsequently, the isotropic and anisotropic chemical shielding (CSI and CSA) parameters have been calculated for the ^{31}P and ^{11}B atoms present in both of the pristine and the C-ring doped structures.

2. Computational methods

In this computational work, the (4,4) armchair BPNTs and C-ring doped model of BPNTs on vertical and horizontal region with 1 nm length (Figs. 1 and 2) have been investigated.

In both models, the mouths of nanotube are saturated by H atoms. All models are individually optimized by using density functional theory (DFT) at B3LYP (Kohn and Sham, 1965; Lee et al., 1988) level of theory using the Gaussian 98 set of programs (Frisch et al., 2001). The standard 6-31G* basis set was used for all models. Calculations were performed on a Pentium-PC computer with a 3000 MHz processor. The chemical shielding (CS) tensors at the sites of ^{11}B and ^{31}P nuclei are calculated based on the gauge included atomic orbital (GIAO) approach (Ditchfield et al., 1971).

The calculated CS tensors in principal axes system (PAS) ($\delta_{33} > \delta_{22} > \delta_{11}$) are converted to measurable NMR parameters, chemical shielding isotropic (CSI) and chemical shielding anisotropic (CSA) by using Eqs. (1) and (2), respectively (Mirzaei, 2010; Schroten et al., 1998; Ferreira and Leite Alves, 2008). The evaluated NMR parameters at the sites of ^{11}B and ^{31}P nuclei in the pristine and C-ring doped models (A and B) are presented in Table 3:

$$\text{CSI (ppm)} = \frac{1}{3}(\sigma_{11} + \sigma_{22} + \sigma_{33}) \tag{1}$$

$$\text{CSA (ppm)} = \delta_{33} - (\delta_{11} + \delta_{22})/2 \tag{2}$$

3. Results and discussion

3.1. The optimized geometries of the BPNTs and C-ring doped

The electronic structural properties of the (4,4) armchair BPNTs and two models of carbon ring doping on horizontal region (model A) and vertical region (model B) (see Figs. 1 and 2) consisting of the B–P bond lengths and B–P–B/P–B–P bond angels are presented in Tables 1 and 2. The results show that the bond lengths for equivalent positions in the three forms of BPNTs are similar. It was shown that when C atoms are substituted in BPNTs, in models (A) and (B), the bond length of B–P is decreased about 1.89 up to 1.46 Å (Table 1). The electronegativity of C (eC = 2.55) is considerably larger than that of B (eB = 2.04) and P (eP = 2.19) leading a charge transfer from B to C yielding asymmetric electronic charge density distribution along CB bond, therefore, the C–P length is shorter than B–P length. This trend would mean that the influence of C-doping instead of the B and P atoms on the properties of the electronic structure of the BPNTs is significant.

In contrast with the same value of bond lengths for different B–P bonds, the bond angles significantly deviate for different bonds. The results of Table 2 show that the value of the bond angle (3–4–11) placed at sides of carbon doped in model (A) is decreased largely from 112° to 99°. Similar results are also observed in C-doped on model (B) for the bond angle (2–1–18) from 122° to 98° and other bond angle such as ([2–3–4], [4–5–6], [13–17–18], [18–17–21], [21–25–26] and [26–25–29]). The bond angle (31–27–28) in model (A) increased from 115° to 129° and this similar trend is shown in model (B) for bond angels (27–28–32) and (30–31–27) from (112° to 124°)

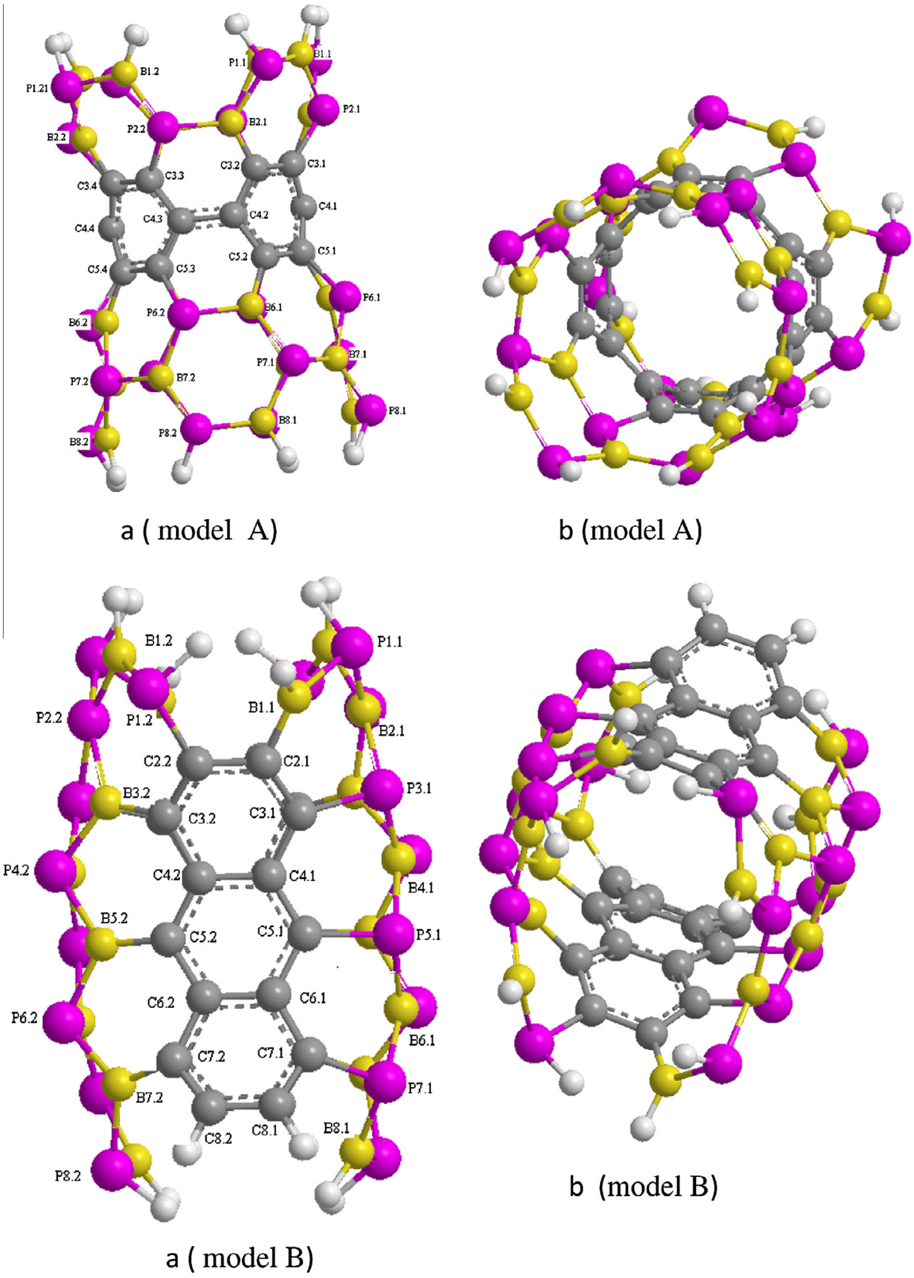

a (model A) b (model A)

a (model B) b (model B)

Figure 2 (a) 2D and (b) 3D views of model (A) and model (B) carbon ring doping in BPNTs.

and (108° to 122°), respectively. Comparison of the results of models (A) and (B) reveal that the deviation in bond angle for vertical ring carbon doped (model B) is larger than horizontal ring carbon doped (model A) in BPNTs. This means that the properties of electronic structures by C-doping in vertical region undergo more changes than C-doping in the horizontal region.

3.2. The NMR parameters of the BPNTs

In this work, we investigated the influences of carbon ring doping in vertical and horizontal region of the BPNTs on the electronic structure properties, the chemical shielding (CS) tensors at the sites of various ^{11}B and ^{31}P atoms are calculated. In order to directly relate the calculated tensors to the experimentally measurable parameters, the tensors are converted to the isotropic CS (CSI) and the anisotropic CS (CSA) parameters. The CSI is the average value of the eigenvalues of the CS tensors, Eq. (1), and the orientation of the eigenvalues of the CS tensors into the z-axis plays a dominant role in determining the value of the CSA parameter, Eq. (2). Table 3 shows the evaluated CSI and CSA values for ^{11}B and ^{31}P in the pristine model of (4,4) armchair BPNTs and two models of C-ring doping (models A and B, Figs. 1 and 2). It shows that the 32 B and 32 P atoms in pristine nanotube of BPNTs is divided into eight layers with equivalent ^{31}P and ^{11}B, NMR parameters for each layer, The results show that the CSI values of layers (1,8), (2,7), (3,6) and (4,5) for B sites are (40, 38, 42 and

Table 1 The optimized geometries of (4,4) BPNT and C-doped.[A].

B–P bonding	Undoped	C-doped		B–P bonding	Undoped	C-doped	
		(a)	(b)			(a)	(b)
Bond length (Å)							
1–2	1.89	1.89	1.96	9–13	1.90	1.44	1.88
2–3	1.91	1.91	1.56	13–17	1.90	1.44	1.90
3–4	1.90	1.91	1.43	17–18	1.90	1.41	1.90
4–5	1.89	1.89	1.90	17–21	1.90	1.89	1.91
5–6	1.89	1.89	1.93	18–22	1.90	1.53	1.40
6–7	1.91	1.91	1.85	19–23	1.90	1.84	1.45
1–8	1.89	1.89	1.89	20–24	1.90	1.53	1.88
7–12	1.91	1.53	1.97	22–23	1.90	1.92	1.46
11–12	1.90	1.42	1.54	21–25	1.90	1.89	1.93
11–15	1.90	1.44	1.48	24–28	1.90	1.91	1.88
14–15	1.90	1.45	1.46	25–26	1.90	1.89	1.91
15–19	1.90	1.45	1.46	26–30	1.90	1.90	1.38
19–20	1.90	1.41	1.53	25–29	1.90	1.91	1.93
16–20	1.90	1.46	1.90	27–28	1.90	1.89	1.54
14–18	1.90	1.46	1.43	27–31	1.90	1.91	1.40
10–14	1.90	1.46	1.46	28–32	1.90	1.90	1.94
9–10	1.90	1.42	1.90	30–31	1.90	1.89	1.40

(a) and (b) are the values of bond length of the C-doping of models A and B.

[A] See Figs. 1 and 2 for details.

Table 2 The optimized geometries of (4,4) BPNT and C-doped.[A]

P–B–P/B–P–P angle	Undoped	C-doped		P–B–P/B–P–P angle	Undoped	C-doped	
		(a)	(b)			(a)	(b)
Bond angles							
2–1–8	122	116	98	16–20–19	111	115	111
1–2–3	108	104	122	17–21–25	117	113	108
2–3–4	122	122	105	18–17–21	122	128	102
2–3–10	115	121	124	19–20–24	111	123	123
3–4–11	112	99	122	20–24–28	121	125	101
4–5–6	122	116	104	21–25–26	121	116	108
5–6–7	108	104	111	22–26–25	111	106	112
6–7–12	115	122	109	22–26–30	115	115	118
7–12–11	113	123	123	22–23–27	113	112	117
9–10–14	122	115	125	23–22–26	121	118	118
9–13–17	111	114	105	24–28–27	121	106	118
10–14–15	122	121	117	25–26–30	112	111	112
11–15–14	111	122	117	26–25–29	124	128	103
12–11–15	122	119	121	26–30–31	123	123	118
13–17–18	122	119	100	27–28–32	112	111	124
14–18–17	111	115	121	30–31–27	108	108	122
15–19–20	122	119	121	31–27–28	115	129	117
15–14–18	122	122	118				

(a) and (b) are the values of bond angles of C-doping of models A and B.

[A] See Figs. 1 and 2 for details.

44 ppm), respectively, and for P sites are (433, 381, 380 and 384 ppm), respectively; which means that the CSI values at the sites of the nuclei of each layer feel equivalent chemical environment.

The CSI values for ^{11}B sites in the C-ring doping of BPNTs in two models (A) and (B) have different trend. So that in model (A) CSI values at the sites of B2.1, B2.2, B6.1, B6.2 and B7.1, B7.2 increased, and in model (B), CSI values at sites B1.2, B1.4 and B3.2 increased and at the other sites of two models decreased.

The CSI values at the site of ^{31}P nuclei in model (A) at all sites increased with respect to the pristine model; the presence of lone pair of electrons in valence shell of ^{31}P caused the significant change more than that at the ^{11}B nuclei. On the other hand, the CSI values for ^{31}P nuclei in model (B) at the sites P1.1, P1.3, P2.2, increased and for other sites decreased with respect to the pristine model. An important point to note is that the CSI values for ^{31}P nuclei in models (A) and (B) at the sites of P7.1 and P1.2, respectively, undergo high significant changes.

Table 3 The NMR parameters of ^{11}B and ^{31}P sites.

B–11 atom	CSI (ppm)			CSA (ppm)			P–31 atom	CSI (ppm)			CSA (ppm)		
	Undoped	C-doped		Undoped	C-doped			Undoped	C-doped		Undoped	C-doped	
		(a)	(b)		(a)	(b)			(a)	(b)		(a)	(b)
B1.1	40	40	37	88	133	94	P1.1	433	462	446	147	130	68
B1.2	40	40	43	88	133	64	P1.2	433	462	395	147	130	100
B1.3	40	–	37	88	–	94	P1.3	433	–	446	147	–	68
B1.4	40	–	43	88	–	64	P1.4	433	–	395	147	–	100
B2.1	38	58	23	83	43	100	P2.1	381	385	–	152	164	–
B2.2	38	58	–	83	43	–	P2.2	381	385	385	152	164	87
B3.1	42	–	–	70	–	–	P3.1	380	–	364	296	–	176
B3.2	42	–	45	70	–	70	P3.2	380	–	–	296	–	–
B4.1	44	–	16	88	–	128	P4.1	383	–	–	163	–	–
B4.2	44	–	–	88	–	–	P4.2	383	–	349	163	–	75
B5.1	44	–	–	79	–	–	P5.1	384	–	391	273	–	218
B5.2	44	–	37	79	–	105	P5.2	384	–	–	273	–	–
B6.1	42	52	14	87	27	117	P6.1	380	395	–	151	171	–
B6.2	42	52	–	87	27	–	P6.2	380	395	368	151	171	67
B7.1	38	52	–	95	47	–	P7.1	382	414	343	276	148	172
B7.2	38	52	33	95	47	82	P7.2	382	414	–	276	148	–
B8.1	40	52	24	109	109	48	P8.1	433	442	–	117	117	54
B8.2	40	39	–	109	109	–	P8.2	433	442	378	–	–	–

In each row, (a) and (b) are the CS values of the C-doping of models A and B. See Figs. 1 and 2 for details.

Since the natures of the CSI and the CSA values are different, their behaviors due to the C-ring doping in the studied BPNTs are also different. The comparison CSA and CSI values show that, CSA values for B nuclei in model (A) at layers B2, B6, B7 decreased with respect to the pristine model. Also the CSA tensors for P nuclei in model (A) at layers P2, P6 increased and at layers P1, P7 decreased. Due to high number of carbons doping in structures of BPNTs in model (B), the CSA values for B nuclei at sites B1.1, B1.3, B2.1, B4.1, B5.2 and B6.1 increased with respect to pristine model, and at the other sites decreased.

The CSA values in model (B) for P atom for all layers decreased with respect to the pristine model.

The CSA values in model (A) and model (B) at the site of B7.1 also undergo notable changes due to the chemical bonding to the B atom and C atom, respectively; therefore, the value of CSA for this nucleus significantly reduces in comparison to that of the pristine model.

The comparison of CSI and CSA values between C-ring doped in model (A) and model (B) reveal that the changes of electrical structures in model (B) are more than model (A), because of more number of carbons doped in the vertical region. It is worth noting that just the electrostatic properties of those nuclei are mainly dependent on electronic density at the sites of nuclei, therefore, due to influence of the C-doping the electronic densities of all nuclei and the CS parameters undergo changes, so the CSI values at all sites that neighbor of C doped undergo notable decrease.

4. Conclusions

We performed density functional theory (DFT) to calculate the CS parameters to investigate the properties and electronic structure of C-ring doping on vertical and horizontal region of the armchair models of (4, 4) BPNTs. The optimized bond lengths reveal that when C atoms are substituted in BPNTs, in models (A) and (B), the bond lengths of B–P is decreased from about 1.89 to 1.46 Å, and the bond angel (3–4–11) placed at sides of carbon doped in model (A) and the bond angle (2–1–18) in model (B) are significantly decreased. The calculated CSI and CSA values for two models reveal that at the site of P7.1 nucleus the electrical structures undergo significant changes because of contributing to the chemical bonding with the C-doping atoms. The results show that the effect of C-ring doping on CS parameters in vertical region model (B) is more sensible than horizontal region model (A).

References

Arenal, R., Ferrari, A.C., Reich, S., Wirtz, L., Mevellec, J.Y., Lefrant, S., Rubio, A., Loiseau, A., 2006. Nano Lett. 6, 1812.

Baughman, R.H., Cui, C.X., Zakhidov, A.A., Iqbal, Z., Barisci, J.N., Spinks, G.M., Wallace, G.G., Mazzoldi, A., De Rossi, D., Rinzler, A.G., Jaschinski, O., Roth, S., Kertesz, M., 1999. Science 284, 1340.

Blase, X., Rubio, A., Louie, S.G., Cohen, M.L., 1994. Europhys. Lett. 28, 335.

Chen, X., Ma, J., Hu, Z., Wu, Q., Chen, Y., 2005. J. Am. Chem. Soc. 127, 17144.

Chopra, N.G., Luyken, R.J., Cherrey, K., Crespi, V.H., Cohen, M.L., Louie, S.G., Zettl, A., 1995. Science 269, 966.

Ditchfield, R., Hehre, W.J., Pople, J.A., 1971. J. Chem. Phys. 54, 724.

Ferreira, V.A., Leite Alves, H.W., 2008. J. Cryst. Growth 310, 3973.

Frisch, M.J., Trucks, G.W., Schlegel, H.B., Scuseria, G.E., Robb, M.A., Cheeseman, J.R., Zakrzewski, V.G., Montgomery Jr., J.A., Stratmann, R.E., Burant, J.C., Dapprich, S., Millam, J.M., Daniels, A.D., Kudin, K.N., Strain, M.C., Farkas, O., Tomasi, J., Barone, V., Cossi, M., Cammi, R., Mennucci, B., Pomelli, C., Adamo, C., Clifford, S., Ochterski, J., Petersson, G.A., Ayala, P.Y., Cui, K., Morokuma, Q., Salvador, P., Dannenberg, J.J., Malick, D.K., Rabuck, A.D., Raghavachari, K., Foresman, J.B., Cioslowski, J., Ortiz, J.V., Stefanov, B.B., Liu, G., Liashenko, A., Piskorz, P., Komaromi, I., Gomperts, R., Martin, R.L., Fox, D.J., Keith, T., Al-Laham, M.A., Peng, C.Y., Nanayakkara, A., Gonzalez, Challacombe, M., Gill, P.M.W., Johnson, B., Chen, W., Wong, M.W., Andres, J.L., Gonzalez, C., Head-Gordon, M., Replogle, E.S., Pople, J.A., . Gaussian 98. Gaussian Inc., Pittsburgh, PA.

Guo, C.S., Fan, W.J., Chen, Z.H., Zhang, R.Q., 2006. Solid State Commun. 137, 549.

Harris, P.J.F., 1999. Carbon Nanotubes and Related Structures. Cambridge University Press, Cambridge.

Kohn, W., Sham, L.J., 1965. Phys. Rev. 140, 1133.

Lee, C., Yang, W., Parr, R.G., 1988. Phys. Rev. B 37, 785.

Li, F., Xia, Y., Zhao, M., Liu, X., Huang, B., Ji, Y., Song, C., 2006. Phys. Lett. A 357, 369.

Loiseau, A., Willaime, F., Demoncy, N., Hug, G., Pascard, H., 1996. Phys. Rev. Lett. 76, 4737.

Mirzaei, M., 2009a. J. Phys. Chem. 223, 815.

Mirzaei, M., 2009b. Physica E 41, 883.

Mirzaei, M., 2010. J. Mol. Model. 17, 89.

Mirzaei, M., Giahi, M., 2010. Physica E 42, 1667.

Mirzaei, M., Hadipour, N.L., Seif, A., Giahi, M., 2008a. Physica E 40, 3060.

Mirzaei, M., Seif, A., Hadipour, N.L., 2008b. Chem. Phys. Lett. 461, 246.

Mpourmakis, G., Froudakis, G.E., 2007. Catal. Today 120, 341.

Nirmala, V., Kolandaivel, P., 2007. J. Mol. Struct. (THEOCHEM) 817, 137.

Oku, T., 2002. Physica B 323, 357.

Schroten, E., Goossens, A., Schoonman, J., 1998. J. Appl. Phys. 83, 1660.

Seif, A., Mirzaei, M., Aghaie, M., Boshra, A., 2007. Z. Naturforsch. 62, 711.

Shen, H., 2009. Comput. Mater. Sci. 47, 220.

Sieh, Z.W., Cherrey, K., Chopra, N.G., Blase, X., Miyamoto, Y., Rubio, A., Cohen, M.L., Louie, S.G., Zettl, A., Gronsky, R., 1995. Phys. Rev. B 51, 11229.

Zhang, D., Zhang, R.Q., 2003. Chem. Phys. Lett. 371, 426.

Zhang, C., Li, R., Zhang, D., Shang, Z., Wang, G., Liang, Y., Xing, Y., Pan, Y., Cai, Z., Zhao, X., Liu, C., 2006. J. Mol. Struct. (THEOCHEM) 765, 1.

Zhou, O., Shimoda, H., Gao, B., Oh, S., Fleming, L., Yue, G., 2002. Acc. Chem. Res. 35, 1045.